Journal of Nuclear Materials 416 (2011) 45–48

Contents lists available at ScienceDirect

Journal of Nuclear Materials

journal homepage: www.elsevier.com/locate/jnucmat

Tungsten–microdiamond composites for plasma facing components

V. Livramento [a], D. Nunes [a], J.B. Correia [a,c,*], P.A. Carvalho [a,b], U. Mardolcar [b], R. Mateus [a], K. Hanada [d], N. Shohoji [c], H. Fernandes [a], C. Silva [a], E. Alves [e]

[a] Associação Euratom/IST, Instituto de Plasmas e Fusão Nuclear, Instituto Superior Técnico, Av. Rovisco Pais, 1049-001 Lisboa, Portugal
[b] IST, Instituto Superior Técnico, Av. Rovisco Pais, 1049-001 Lisboa, Portugal
[c] LNEG, Laboratório Nacional de Energia e Geologia, Estrada do Paço do Lumiar 22, 1649-038 Lisboa, Portugal
[d] National Institute of Advanced Industrial Science and Technology (AIST), 1-2-1 Namiki, Tsukuba, Ibaraki 305-8564, Japan
[e] ITN, Instituto Tecnológico e Nuclear, Estrada Nacional 10, 2686-953 Sacavém, Portugal

ARTICLE INFO

Article history:
Available online 24 February 2011

ABSTRACT

Tungsten is considered as one of promising candidate materials for plasma facing component in nuclear fusion reactors due to its resistance to sputtering and high melting point. High thermal conductivity is also a prerequisite for plasma facing components under the unique service environment of fusion reactor characterised by the massive heat load, especially in the divertor area. The feasibility of mechanical alloying of nanodiamond and tungsten, and the consolidation of the composite powders with Spark Plasma Sintering (SPS) was previously demonstrated. In the present research we report on the use of microdiamond instead of nanodiamond in such composites. Microdiamond is more favourable than nanodiamond in view of phonon transport performance leading to better thermal conductivity. However, there is a trade off between densification and thermal conductivity as the SPS temperature increases tungsten carbide formation from microdiamond is accelerated inevitably while the consolidation density would rise.

1. Introduction

There has been growing interest in the nuclear fusion reactor as a very long-term option for the future energy source. However, one of the major obstacles to construct a commercial fusion reactor is the lack of acceptable first-wall materials that will allow competitive operating temperatures with the maximized service life of the fusion reactor. There are a number of technical specifications to be fulfilled by the plasma facing components including high thermal conductivity, thermal stability, resistance to radiation induced defects and medium temperature toughness [1]. A new composite material, tungsten–microdiamond (W–microdiamond), is investigated in the present research. The extremely high thermal conductivity of diamond enables the tailoring of properties in such composites. Additionally, microdiamond is an excellent reinforcing and stabilization candidate, judging from the experimental evidence acquired for tungsten–nanodiamond (W–nanodiamond) composites as well as for copper–nanodiamond (Cu–nanodiamond) composites [2–7].

Refractory metals in general, and tungsten in particular, are currently under intense investigation for this application due to their high resistance to plasma erosion and moderate tritium retention [8]. The fine grain structure induced via mechanical alloying can improve room temperature ductility [9]. However, further enhancement in thermal conductivity, thermal stability and room temperature ductility are demanded for these materials. An improved performance is also desirable and alternative solutions are sought for long term improvement. As an alternative, W–microdiamond composites are promising candidates for thermally stable first-wall materials for fusion reactors. Polycrystalline diamond coatings have previously been exposed to fusion plasma and subsequently characterised. It was demonstrated that diamond coating could withstand the high heat fluxes generated by fusion plasmas with the benefit of improved heat extraction [10]. However, the irradiation resistance of W–microdiamond composites as well as on the highest upper operation temperature that might be tolerable probably preclude the use in DEMO where the upper operation temperature is typically 1775 K (e.g. in helium cooled divertors) but may find application in ITER where requirements are less stringent.

A major challenge with mechanical alloying (MA) of this material is the strong affinity of tungsten towards carbon, leading to the undesired formation of carbides. This problem was solved for W–nanodiamond using a low level of energy during MA [2].

* Corresponding author at: LNEG, Laboratório Nacional de Energia e Geologia, Estrada do Paço do Lumiar 22, 1649-038 Lisboa, Portugal. Tel.: +351 210 92 4660; fax: +351 217 163 688.
E-mail address: brito.correia@lneg.pt (J.B. Correia).

0022-3115/$ - see front matter © 2011 Elsevier B.V. All rights reserved.
doi:10.1016/j.jnucmat.2011.02.031

Tungsten–microdiamond composites were prepared by MA using a low milling energy input, benefiting from experience gained with W–nanodiamond processing, and were subsequently consolidated by Spark Plasma Sintering (SPS).

2. Materials and methods

Different batches of W–microdiamond were produced by MA, using mixtures of powders: W–40% at microD. Pure elemental W was used as the matrix (purity 99.95%; median particle size 1 μm) and microdiamond powders with several different sizes (10, 50 and 100 μm) from Sumiseki Materials Co., were used as the reinforcement agent for the matrix. The milling was performed during 2 and 4 h for all the 3 different batches (W–40% at microD_10 μm; W–40% at microD_50 μm and W–40% at microD_100 μm). The millings were carried out in a Retsch PM400 planetary ball mill, using WC balls with a diameter of 10 mm in 250 ml WC containers. The batch milling charge was constituted by 19.17 g of W and 0.83 g of microD. The mill rotation speed was 200 rpm.

All the powder batches were characterized by X-ray diffraction (XRD: Cu Kα radiation, 0.8°/min, step 0.04) using a Rigaku Geigerflex D/MAX III C diffractometer; optical microscopy; field emission scanning electron microscopy (SEM) with energy dispersive X-ray spectroscopy analysis (EDS), using a Philips XL30 FEG fitted with EDS EDAX Sapphire (SUTW) detector; and differential thermal analysis (DTA) was carried out for all the batches, using TGA/DTA Labsys (Setaram) equipment. The heating and cooling rates were 293 K min^{-1}. and the samples were protected by purging with inert Ar gas during the runs. Thermal diffusivity measurements were performed with a laser flash instrument, FlashLine 5000 Anter Corporation.

The milled powders consolidated with SPS at several temperatures (1073 K, 1123 K, 1273 K and 1423 K). The consolidated samples were characterized by geometric density and thermal diffusivity. Microhardness value for each consolidated sample was obtained with a Vickers indenter in a Shimadzu HMV 2000 hardness tester using a load of 0.49 N for 15 s (ISO 6507-1). XRD analysis, SEM microstructure observation and SEM/EDS chemical analyses were also made for the consolidated samples.

3. Results and discussion

The milling at 200 rpm, both for 2 and 4 h, prevented W carbides formation, as evidenced with XRD. The only peaks clearly identifiable in as-milled samples were those of W, Fig. 1. Also the amount of WC contamination from the milling media is very small. Diamond peaks are absent due to the low diffraction yield of carbon relative to that of the much heavier element W.

Fig. 2 shows the microstructure of W–40% at microD (10 μm) powder composite after milling at 200 rpm. The microstructure is

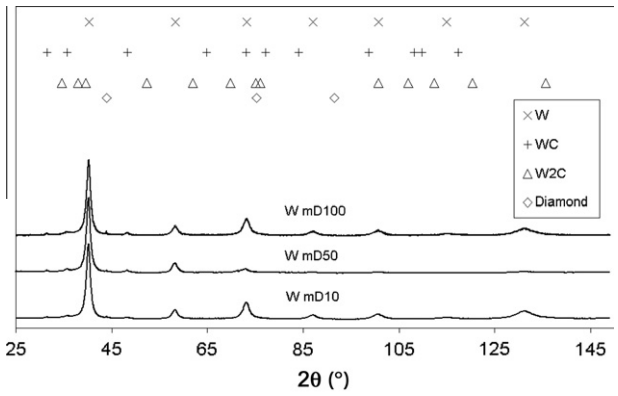

Fig. 1. XRD patterns for all W–40% at microD samples milled for 4 h at 200 rpm.

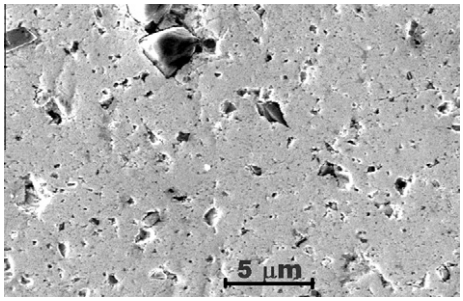

Fig. 2. SEM picture of W–40% at microD (10 μm) after mechanical alloying for 2 h at 200 rpm.

relatively heterogeneous, with different sizes of microdiamond particles. The diamond particles are reduced in size due to fracture during the milling process. A longer milling period of 4 h produced a more uniform size distribution, as shown in Fig. 3. This condition was also used for the samples processed by the SPS consolidation.

The thermal analyses of all batches yielded similar results. Fig. 4 shows the results for the W–40% at microD (100 μm) sample milled at 200 rpm. The pristine mixture without milling shows a small endothermic peak at about 1423 K, probably associated with the graphitisation of diamond. The samples milled at 200 rpm show a strong endothermic peak associated with W carbide formation in the range 1243–1253 K. This peak tends to shift towards lower temperatures for longer milling times indicating that the energy input from the MA process promotes the reaction of diamond with tungsten. The formation of both types of carbide W_2C and WC after DTA is clearly shown in Fig. 5.

The densification results obtained after SPS consolidation are presented in Table 1.

Fig. 6 presents SEM pictures of the sample consolidated by SPS at 1273 K (W–40% at microD (50 μm) at 200 rpm, milled for 4 h). It is possible to observe a satisfactory densification of the material. The surface (a) is rich in carbon than the interior (b) owing to graphite from SPS tooling. The geometric density of this sample was 77% and the microhardness of this material is 13.67 ± 2.79 GPa. The low density of the materials consolidated below 1273 K did not allow proper hardness measurements. Higher densification is mandatory for fusion applications. This could be achieved in the future with hammer forging to increase density and ductility. Increasing the consolidation temperature it is possible to obtain higher densification of the powders, and thus the microhardness after SPS at 1423 K (W–40% at microD (50 μm) – 4 h at 200 rpm) was 23.90 ± 0.82 GPa. This higher value may also reflect the larger extent of W carbide formation at higher temperatures.

Fig. 7 shows the thermal diffusivity of all SPS consolidated samples of W–40% at microD (50 μm) at 200 rpm, milled for 4 h. The thermal conductivity is proportional to density in a porous material. Therefore increasing the consolidation temperature appeared to contribute towards the enhanced densification of the powders, and subsequently to the enhanced thermal diffusivity. However, we observe an inversion above 1123 K, e.g. the thermal diffusivity of SPS samples consolidated at 1423 K and 1073 K have similar values although their respective densities are 56% and 88% of the theoretical density. The fast carbide formation at 1243 K detected via DTA, Fig. 4, is responsible for the loss of the high conductivity diamond structure at the consolidation temperatures, 1273 K and 1423 K.

The highest thermal diffusivity values measured in this research are about 8×10^{-6} m^2 s^{-1} albeit in a very porous body (only 66% of the theoretical density with the consolidation temperature of 1123 K). Owing to extensive porosity these values of thermal diffusivity are of course lower than that of bulk tungsten, about 7×10^{-5} m^2 s^{-1} at room temperature, but still larger than those

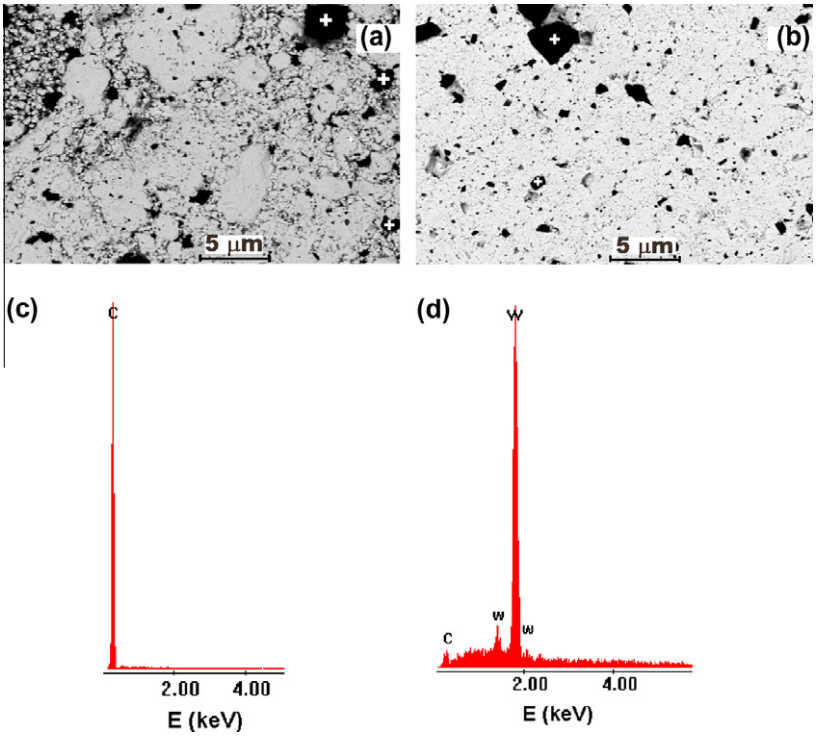

Fig. 3. SEM/BSE Images of W–40% at microD (10 μm) at 200 rpm, milled for different times (a) 2 h and (b) 4 h, and typical EDS analyses (c) dark particles, marked with + in pictures and (d) brighter matrix.

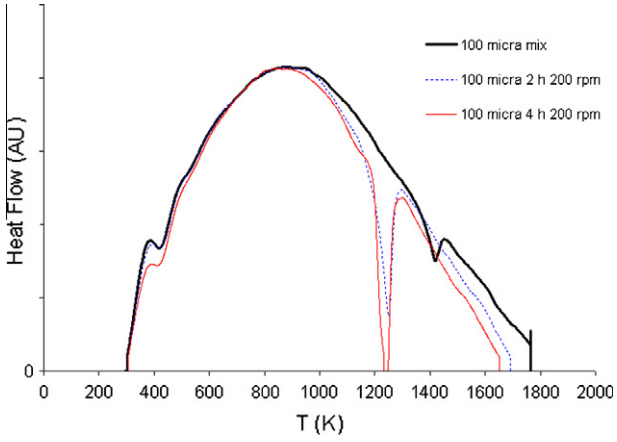

Fig. 4. DTA of W–40% at microD (100 μm) 200 rpm, just mixed, and after 2 and 4 h milling.

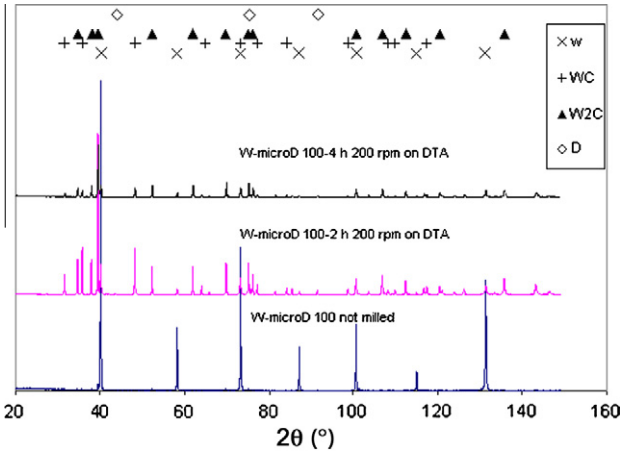

Fig. 5. XRD patterns after DTA of W–40% at microD (100 μm) 200 rpm, without milling, and after 2 and 4 h milling.

obtained for thermal sprayed tungsten having a smaller porosity [11]. A porosity level of more than 30% can of course account for the substantial reduction in thermal diffusivity relative to a 100% dense body through the Maxwell–Eucken model.

The present work shows that milling at 200 rpm for 4 h followed by SPS at 1423 K represents the best combination of processing parameters to obtain maximum densification (88%). However, a consolidation temperature below 1273 K must be used in order to maintain a W–microdiamond composite, with high thermal conductivity, and avoid W carbide formation.

4. Conclusions

In summary, it is possible to perform mechanical alloying of W at 200 rpm with different sizes of microdiamond powders at room temperature without major W carbide formation. Also, the use of a short milling time of only 2 and 4 h provided a favourable condition for a small degree of the contamination from the milling tool during mechanical alloying.

The present work shows that the higher SPS consolidation temperature, 1423 K, is best for obtaining high density in the

Table 1
Densification results of W–40% at microD (50 μm) milled 4 h at 200 rpm.

SPS temperature (K)	Density (g cm^{-3})	Theoretical density (%)
1073	9.1	56
1123	10.8	66
1273	12.6	77
1423	14.3	88

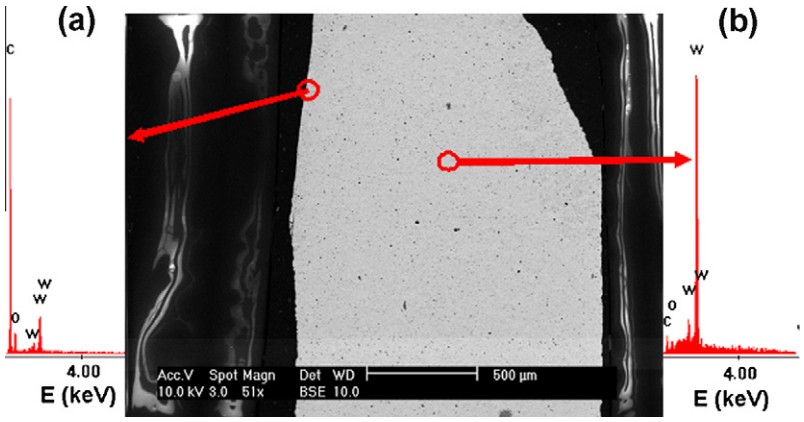

Fig. 6. SEM Image and EDS analysis of W–40% at microD (50 µm) at 200 rpm, milled for 4 h after SPS at 1273 K.

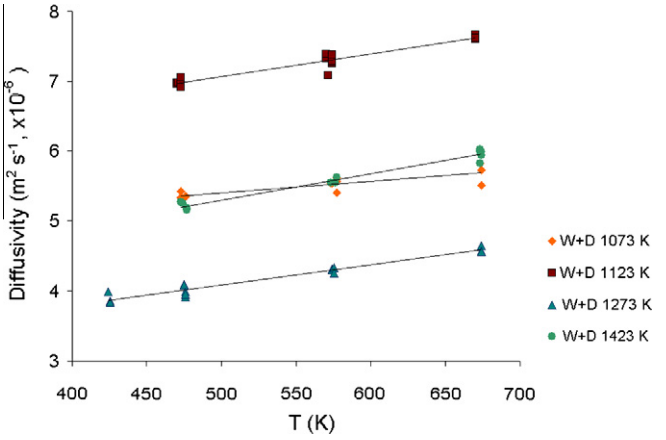

Fig. 7. Thermal diffusivity after SPS of samples of W–40% at microD (50 µm) milled for 4 h at 200 rpm.

consolidated samples. However, for preserving the diamond structure, with high thermal diffusivity, in the W–microdiamond composite and avoid W carbide formation, SPS temperature must be below 1273 K. Hammer forging at temperatures below 1273 K of SPS consolidated samples would be a suitable way to increase substantially the density and thermal conductivity but also the ductility with the perspective for structural applications of W–microdiamond.

References

[1] A.R. Raffray, R. Nygren, D.G. Whyte, S. Abdel-Khalik, R. Doerner, F. Escourbiac, et al., Fusion Eng. Des. 85 (2010) 3–108.
[2] D. Nunes, V. Livramento, J.B. Correia, R. Mateus, P.A. Carvalho, N. Shohoji, H. Fernandes, C. Silva, E. Alves, K. Hanada, E. Osawa, Mater. Future Fusion Fission Technol. 1125 (2009) 59–64.
[3] J. Correia, V. Livramento, N. Shohoji, E. Tresso, K. Yamamoto, T. Taguchi, K. Hanada, E. Osawa, Adv. Mater. Forum IV 587–588 (2008) 443–447.
[4] K. Hanada, K. Yamamoto, T. Taguchi, E. Osawa, M. Inakuma, V. Livramento, J. Correia, N. Shohoji, Diam. Relat. Mater. 16 (2007) 2054–2057.
[5] V. Livramento, J. Correia, D. Nunes, P. Carvalho, H. Fernandes, C. Silva, K. Hanada, N. Shohoji, E. Osawa, Plasma Fusion Sci. 996 (2008) 166–171.
[6] V. Livramento, J. Correia, N. Shohoji, E. Osawa, Diam. Relat. Mater. 16 (2007) 202–204.
[7] K. Yamamoto, T. Taguchi, K. Hanada, E. Osawa, A. Inakuma, V. Livramento, J. Correia, N. Shohoji, Diam. Relat. Mater. 16 (2007) 2058–2062.
[8] M. Ubeyli, S. Yalcin, J. Fusion Energy 25 (2006) 197–205.
[9] Y. Ishijima, S. Kannari, H. Kurishita, M. Hasegawa, Y. Hiraoka, T. Takida, K. Takebe, Mater. Sci. Eng. A Struct. Mater. 473 (2008) 7–15.
[10] S. Porro, G. De Temmerman, P. John, S. Lisgo, I. Villalpando, J.I.B. Wilson, Stat. Solid A 206 (2009) 2028–2032.
[11] H.K. Kang, J. Nucl. Mater. 335 (2004) 1–4.